Controlled-STM: A Two-stage Model to Predict User's Perceived Intensity for Multi-point Spatiotemporal Modulation in Ultrasonic Mid-air Haptics

Zhouyang Shen
zhouyang.shen.21@ucl.ac.uk
University College London
London, United Kingdom

Zak Morgan
zak.morgan.17@ucl.ac.uk
University College London
London, United Kingdom

Madhan Kumar Vasudevan
madhan.vasudevan@ucl.ac.uk
University College London
London, United Kingdom

Marianna Obrist
m.obrist@ucl.ac.uk
University College London
London, United Kingdom

Diego Martínez Plasencia
d.plasencia@ucl.ac.uk
University College London
London, United Kingdom

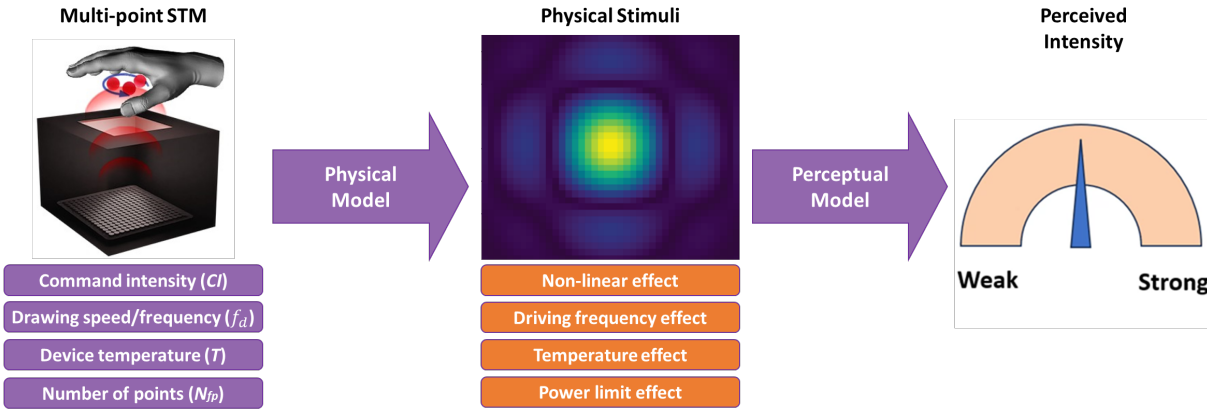

Figure 1: We propose a 2-stage model to predict perceived intensity for multi-point STM haptics. The *physical model* (left arrow) predicts the physical properties of the stimuli (e.g., pressure, force), from the modulation parameters used (e.g., command intensity, Drawing frequency, device temperature and number of points); The *perceptual model* (right arrow) then predicts the perceptual response taking into account the physical properties of the stimuli.

ABSTRACT

Multi-point STM offers a great range of parameters (i.e., drawing frequency, number of points) to produce different tactile sensations. However, existing studies offer limited insight on the effects of these parameters, and ignore their effect on the physical stimuli delivered, limiting effective haptic design. We propose a two-stage model to predict response to multi-point STM. The first stage predicts physical stimulus properties with 7.8% error, while the second stage predicts mean and spread of perceived intensity with 8.0 % and 8.8% error. We report 3 studies conducted to derive this model: one to characterize physical stimuli, another one measuring user perceptual thresholds, and a third one measuring user's perceptual response to multi-point STM. Besides, we characterize 4 effects that influence device performance, confirm if previous effects reported are due to physical or perceptual effects (or both) and derive recommendations for manufacturers, haptic designers and HCI researchers.

CCS CONCEPTS

• **Human-centered computing** → **Haptic devices**; *User studies*; *User models*.

KEYWORDS

mid-air haptics, perception, polynomial regression

ACM Reference Format:
Zhouyang Shen, Zak Morgan, Madhan Kumar Vasudevan, Marianna Obrist, and Diego Martínez Plasencia. 2024. Controlled-STM: A Two-stage Model to Predict User's Perceived Intensity for Multi-point Spatiotemporal Modulation in Ultrasonic Mid-air Haptics. In *Proceedings of the CHI Conference on Human Factors in Computing Systems (CHI '24), May 11–16, 2024, Honolulu, HI, USA.* ACM, New York, NY, USA, 12 pages. https://doi.org/10.1145/3613904.3642439

CHI '24, May 11–16, 2024, Honolulu, HI, USA

ACM ISBN 979-8-4007-0330-0/24/05
https://doi.org/10.1145/3613904.3642439

1 INTRODUCTION

Multi-point Spatiotemporal Modulation (STM) uses one or more points of focused ultrasound (i.e., focal points) quickly moving along the users' skin to create tactile sensations [11, 55]. Several parameters have been found to affect how users perceive STM stimuli, such as drawing frequency (f_d) [11, 38], the way the shape is discretised [12] or the number of points (N_{fp}) used [55].

However, all prior studies directly map the effect of such high-level STM parameters (e.g., drawing frequency) to users' perceived intensity (*PI*), without paying any regard to the effect these high-level parameters could have on the physical properties of the stimuli being delivered (e.g., pressure/force of each point).

As such, it remains unclear if the differences found are indeed the result of the users' perceptual response (e.g., tactile receptors) or due to the physical properties of the stimuli (e.g, stronger/weaker focal points). Similarly, the physical properties that better determine users' response remain unclear (e.g., pressure or force?; in absolute terms or relative to users' perceivable thresholds?).These uncertainties impede designers from predicting the effect of the tactile stimuli they craft, and limit HCI researchers' insights into how humans respond to multi-point STM.

We address these limitations by constructing a two-stage model: The first stage characterizes the physical properties of the focal points (e.g., peak pressure, forces) from the input parameters (i.e., number of points used, drawing speed/frequency, intensity and temperature). The second stage builds on these properties to predict the perceptual response on the user.

This approach allows us to decouple physical and perceptual responses, gaining understanding on the parameters that affect the physical stimuli (i.e., due to device's artefacts/limitations), but also the parameters and physical properties that drive users' response to multi-point STM (i.e., human perception). While the first part might vary from one device to another, the second one only depends on the users' response to a given physical stimuli and could be reusable across devices/manufacturers.

We conducted 3 experiments in order to construct our model. The first study measured the physical stimuli delivered by an OpenMPD device [41], as input parameters changed (e.g., command intensity (*CI*), number of points (N_{fp}), drawing frequency (f_d) and temperature (T)), and explored their relationships to produce our *physical model* (i.e., first stage). To model the physical stimuli relative to users' perceivable thresholds, we conducted a second study measuring participants' minimum perceivable thresholds for STM at several drawing frequencies. Finally, our third study consisted of a magnitude estimation task, with varying number of points, intensities and drawing frequencies.

We derive our model from these studies, built as a simple combination of analytical expressions to: 1) predict the acoustic pressure under different CI, f_d, N_{fp} and T conditions with an average relative error of 7.8%; 2) predict users perceived intensity based on f_d, N_{fp} and the physical properties predicted from the *physical model*, with an average relative error of 8.0%.

Our model and study results allow us to derive recommendations for several audiences, such as device manufacturers (i.e., effects hindering devices' response, and their relative relevance), haptic designers (i.e., use our model as a potential tool to predict users' response and inter-subject variability, while they are designing the stimuli) and HCI researchers (i.e., insights on human response to multi-point STM).

2 RELATED WORK

Ultrasonic mid-air haptics (UMH) renders haptic sensation through focused ultrasound, delivered via Phased Arrays of Transducers (PATs). Each transducer is driven with a phase delay such that the waves of all transducers converge on the same point and at the same time, creating a point of high pressure (i.e., a focal point [6]).

Modulation techniques are required to make such points perceivable [55]. Amplitude Modulation (AM) changes the intensity (i.e., pressure) of each focal point over time [21], while Lateral Modulation (LM) retains focal points active at all times, using small lateral oscillations to make them perceptible [47]. Spatiotemporal Modulation (STM) leverages focal points moving quickly along a tactile shape, either using one [11, 28] or many [39, 55] points.

Our review focuses on STM techniques. First we describe studies exploring the perceptual response to STM stimulation. Second, we focus on the effects STM parameters can have on the physical stimuli. Third, we summarize prior studies describing how physical properties of the stimuli affect perceived intensity (*PI*).

2.1 Perceptual response to STM haptics

The acoustic pressure (Pa) of each focal point is arguably the most defining parameter determining the intensity of the stimuli, and algorithms exist controlling the intensity of each point [31, 39].

However, the way those points interact with users' skin is similarly relevant. Frier et al. [11] found a quadratic relationship between *PI* and the speed of the STM point (i.e., drawing speed V_d or frequency f_d, both terms are interchangeable [39]). Similarly, the way the tactile shape is sampled (e.g., points along the shape, time spent at salient points) have also shown to affect *PI* [12, 34].

Finally, the number of points (N_{fp}) used to render the shape have also been shown to affect *PI* [55], along with other emotional responses. Other studies have further looked into the effects of STM on emotional responses (e.g., [3, 37]), but this paper will limit its focus to predicting *PI*.

In summary, prior literature has shown how several parameters influence *PI*, namely: Command Intensity (*CI*, target pressure for each focal point (in Pa) requested to the algorithm); Drawing frequency (f_d, number of times each focal point traverses the shape per second); Number of Points used (N_{fp}) and sampling (location and timing of focal points along the shape).

However, none of these studies looked into the effects that changing such parameters had on the physical stimuli delivered (e.g., pressure of the focal points, forces). They all attribute the effects observed strictly to users' perceptual response, without considering if the physical stimuli used for their comparisons are, indeed, comparable. As such, it is not currently possible to assess if such effects are due to users' perceptual response, or to the way the physical stimuli is delivered by the PAT device. This direct mapping also triggers generalization problems. For instance, Ablart et al. [2] concluded that drawing speeds of 12.5 m/s introduced higher perceived intensity than 10 m/s, while this result was the opposite in [11].

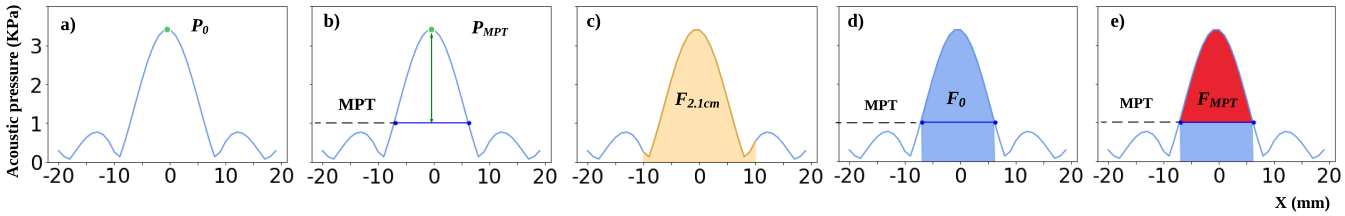

Figure 2: Physical properties of a focal point considered (for multi-point, we use summation of individual points' properties): a) Peak pressure, relative to room pressure (P_0); b) Peak pressure, relative to users' MPT (P_{MPT}); c) Force across 2.1 cm area ($F_{2.1}cm$); d) Absolute force across the area perceivable to user (F_0); e) Force across perceivable area and relative to users' MPT (F_{MPT}).

Thus, it further encouraged us to study the underlying physical effect of parameters on perceived intensity to ensure reliable delivery of the haptic experiences.

2.2 STM parameters and the physical stimuli

There are a number of effects that can affect the physical stimuli (i.e., the focal points) delivered by PATs , such as *non-linear effects*, *limited power*, sub-optimum *driving frequencies* of the transducers or *transducers' temperature*. We here discuss such effects and how the STM parameters used can influence them.

Non-linear acoustics is a branch of physics which comes into play when dealing with high amplitude waves [32]. Linear models do not apply in these cases and such systems are governed by fluid dynamics instead.

Existing STM algorithms [31, 39], however, rely on linear acoustics and analytical models of transducers' directivity (e.g., piston model [41]), to determine the acoustic pressure delivered. While the directivity and intensity of each individual transducer has been experimentally validated by several works [19, 35], the joint contribution of all transducers in the PAT could (and does, as show later in the paper) lead to sufficiently high pressures for *non-linear effects* to appear. As such, STM solvers could attempt to produce intensities (CI) beyond the linear regime, and fail to predict the intensity of the focal points they are actually creating.

Secondly, the PAT is limited in terms of the acoustic power that it can deliver, but the underlying algorithm can still attempt to create focal point intensities beyond such *limited power* (i.e., the actual focal point would be weaker than the intended CI requested to the solver). This is particularly complex if several points (N_{fp}) are being created. In this case, the designer would need to retain a notion of *feasible* $CI's$, per number of points used, or resort to tools to assess that the algorithm can indeed achieve such intensities.

Thirdly, the high update rate of STM algorithms can lead to sub-optimum *driving frequencies* of the transducers. Transducers are narrow-band electro-mechanical actuators, designed (in most PATs) to operate at 40 KHz. At the same time, STM algorithms require update rates [11, 39] in the same order of magnitude than this frequency (e.g., 10 K updates/s vs 40 KHz transducers' frequency). Each update forces a change in phase every few cycles (i.e., 4 cycles, in our example), forcing transducers to operate outside of their resonant frequency and leading to loss of acoustic power [50].

The larger the phase change required per update, the higher the power loss will be, and several STM parameters can require such high phase changes. Higher speeds (V_d or f_d) will require more aggressive phase changes, as the phase change depends on each points' displacement relative to the transducer [19]. The use of several points (N_{fp}) will also require phase-retrieval methods [39], involving less predictable phase updates.

Finally, these same reasons can affect *transducers' temperature*. The impedance of transducers can be matched for specific frequencies [13], leading to minimum power consumption and heat dissipation. Operating outside the nominal frequency, however, would still result in higher consumption and heat. Such temperature changes directly affect transducers' output and resonant frequency [50], reducing the performance and accuracy of the PAT.

2.3 Physical stimuli and perceived intensity (PI)

There are prior works exploring perceptual responses to vibrotactile stimuli [18, 22, 52]. However, most of them focus on contact-based actuators (e.g., vibrators), and it remains unclear if such findings are transferable to multi-point STM.

As indicated earlier, most studies focus on the effects that STM parameters have on PI, not considering the physical properties of the stimuli. As such, the physical properties of the STM stimuli (see Figure 1.centre for a typical pressure distribution of a focal point) that better determine PI are not widely understood.

Some studies use the peak pressure of the points (i.e., summation) as an estimate of the intensity of the tactile stimuli (i.e., see P_0, in Figure 2.a). In GS-PAT [39], authors used this metric to argue that a small number of points (N_{fp}) should provide similar STM quality than a single point, but with no actual validation. A later study on multi-point STM [55] disregarded such hypothesis (i.e., PI was higher for $N_{fp} = 1$), and suggested that considering the peak pressure relative to users' minimum perceivable threshold (MPT) [18] could be a better predictor (see P_{MPT}, in Figure 2.b).

Although not specific from STM, other approaches [10] focus on the acoustic force (i.e., pressure integrated over unit area) delivered by the stimuli. More specifically, they used a force scale with a sensing plate of $2.1cm$ in diameter, comparing such direct measurements with their force estimations across such area (see $F_{2.1cm}$, in Figure 2.c), but without validating its actual correlation with PI. Alternatively, knowledge of the users' MPT for STM stimulation could allow for more refined estimations, integrating force only along the area perceptible to the user, either in absolute or in relative terms (i.e., F_0 and F_{MPT} respectively, in Figures 2.d&e).

Some works also look into the effects of ultrasound stimuli on the users' skin [10], considering their rheological properties to model other effects, such as indentation [11]. We however limit our

exploration to characterizing the stimuli, and the properties that better predict *PI* (i.e., P_0, P_{MPT}, $F_{2.1cm}$, F_0 and F_{MPT}, in Figure 2; Refer to Supplementary Material to see how all these properties can be derived from the pressure distribution and P_0).

3 CONTROLLED-STM: SUMMARY OF APPROACH

Our core contribution is the description of a predictive model for Perceived Intensity (*PI*) for Multi-Point STM stimulation, addressing all modulation parameters (i.e., N_{fp}, CI and f_d, approach summarised in Figure 1). As a main distinctive point, we do this by looking at the effects of such parameters both on the physical properties of the STM stimuli and on the users' perceptual response, providing insights on which effects are the result of the way the device delivers the stimulation and which ones are inherent to users' perceptual response to STM stimulation.

This approach results is a two-stage model: a *Physical Model* characterizing the way STM parameters influence the stimuli, and a *Perceptual Model* predicting users' *PI* from the stimuli's parameters. More specifically, the *Physical Model* is composed of two components. The first one $P_0(CI, N_{fp}, f_d, T)$ (extracted from Study 1) predicts the peak acoustic pressure of each point (i.e., P_0, in Figure 2) from our STM parameters and the device's temperature (T), as a combination of several functions: *non-linear effects* (*NL*), *driving frequencies* (*DF*), *transducers' temperature* (*TT*) and *limited power* (*LP*), with each function representing a corresponding physical effect affecting device's performance. Here, P (or $P_{CI=6531,static,T=31}$) represents the pressure measured for a single static focal point at CI=6531 and T=31°C (i.e., default case):

$$P_0(CI, N_{fp}, f_d, T) = \begin{cases} P \cdot \frac{NL(CI)}{NL(6531)} \cdot \frac{DF(f_d)}{DF(0)} \cdot \frac{TT(T)}{TT(31)} & \text{if } N_{fp} = 1 \\ P \cdot \frac{LP(CI,N_{fp})}{LP(6531,1)} \cdot \frac{DF(f_d)}{DF(0)} \cdot \frac{TT(T)}{TT(31)} & \text{if } N_{fp} > 1 \end{cases} \quad (1)$$

The second component of the *Physical Model* is $MPT(f_d)$, describing users' minimum perceivable threshold to STM stimuli, as a function of f_d (extracted from Study 2). This function is retained as part of the *Physical Model* as such thresholds are required to extract the properties described in Figure 2 (i.e., particularly P_{MPT} and F_{MPT} are relative to *MPT*), but $MPT(f_d)$ indeed plays a pivotal role between the physical and perceptual stages.

The *Perceptual Model* (i.e., second stage) is composed of two functions: i) *PM*, predicting average Perceived Intensity (*PI*); and, ii) PM_{STE} predicting the variance (standard error) of *PI* across users. They both depend on P_{MPT}, f_d and N_{fp}, as extracted from Study 3:

$$PI(CI, N_{fp}, f_d, T) = PM(P_{MPT}, f_d, N_{fp}) \quad (2)$$

$$PI_{STE}(CI, N_{fp}, f_d, T) = PM_{STE}(P_{MPT}, f_d, N_{fp}) \quad (3)$$

The following sections detail each stage, describing the 3 studies conducted to construct our model, as well as the analysis of results, effects observed and rationale that led to this design.

4 PHYSICAL MODEL

The *physical model* aims to characterise the properties of the physical stimuli delivered, when different STM parameters are used (i.e., CI, N_{fp}, f_d, T). The results from Study 1 provide an estimation of the acoustic peak pressure of each point (i.e., P_0) which, together with the *MPT*s obtained in Study 2, allows us to derive all the other properties in Figure 2 (see Supplementary Material).

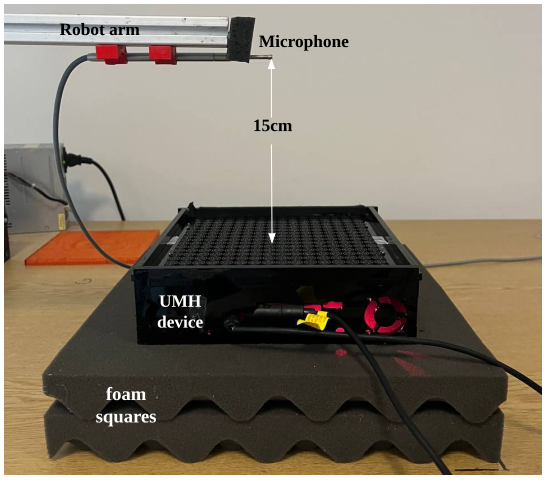

Figure 3: Measuring setup used to characterize P_0 delivered by the device as STM parameters were varied, featuring a PAT device and a measuring microphone on a moving stage.

4.1 STUDY 1: From STM parameters to P_0

4.1.1 *Experimental Design*.

We used the open-source platform OpenMPD [41] for all our tests, both for software (GS-PAT algorithm, at 10 KHz) and hardware (PAT with 256 transducers working at 40 KHz, operated at 18 V), modified by adding a DS18B20 temperature sensor to the back of the PAT to collect temperature readings. We used this setup to create different multi-point STM stimuli, measuring the resulting pressure as we varied all 4 parameters affecting device performance (CI, f_d, N_{fp} and T).

More specifically, we measured intensities (CI's) in a range from 544 Pa to 6531 Pa, with the latter being the highest achievable CI that the solver can deliver to a single focal point. We explored drawing frequencies f_d = {5, 10, 20, 40, 80, 120, 160, 240, 320 Hz}, as to cover the sensitive range of both Meisnner and Pacinian mechanoreceptors [18]. We limit our exploration to N_{fp} = {1,2,3} points, as both physical measurements [39] and prior studies [55] indicate significant decreases in performance past this number of points. Finally, we characterised the PAT's performance as temperature increased from 25°C (room temperature) to 50°C (safe upper limit). We fixed the remaining STM parameters to avoid confounding factors. The height of the focal point was fixed at 15 cm from the device as to avoid changes in pressure related to location [10, 39, 40]. We use a circular pattern (i.e., as to avoid salient points/corners' influence [34]) of 6.5 cm (within the typical size of an adult's palm of 7.5—9.5 cm [30]), discretised using 100 positions homogeneously sampled along the circle shape (i.e., avoid timing effects [34]). It must be noted that for higher f_d > 100 Hz, it is impossible to render the shape with 100 positions (i.e., at 320 Hz, one can only use $\frac{10KHz}{320} \approx 31$ samples). However, Frier et al. [12] found that *PI* is

not significantly affected by the number of samples for such high frequencies, so we did not consider the difference in sampling rate as a confounding factor in these cases.

4.1.2 *Measurement setup and procedure.*

The measurement device setup is shown in Figure 3. The PAT was placed above foam squares to absorb environment vibrations during our tests. A motorized stage (i.e., CNC machine) was used to place a Bruel & Kjaer 1/8" Type 4138 Pressure-field Microphone at one point of our STM circle (i.e., (0mm, 31mm, 150mm)). A small search was performed over an area of 8x8 mm to ensure the microphone was placed at the point of maximum pressure (i.e., right on top of our haptic shape). The microphone was connected to a PicoScope sampling at 10 MHz, and each test recorded enough samples as to capture a full revolution of all focal points around the circle (i.e., 10 MHz/f_d samples), and each measurement was repeated 3 times.

As per the microphone data-sheet[29], a free-field measurement is approximated from the pressure response using the included graph, and 0.78 dB is subtracted from the measurements, as the sound is measured at a 90 degree angle to the microphone tip. This accounts for the increase in pressure due to diffraction of the sound waves around the microphone.

We report 4 experiments, each characterizing one of the 4 physical effects affecting the device's performance described in Related Work. For each effect, we only varied (and measured) the parameters influencing said effect, retaining other (independent) parameters fixed. More specifically, we consider the case of a single, fixed focal point as a default case (i.e., CI=6.5 KPa, N_{fp}=1, f_d=0 Hz, T=31°C), and use these parameters as the default fixed values for the independent parameters, as we explore the influence of varied parameter on the physical stimuli studied. However, for the LP effect, it is constructed differently than other effects as the effect of N_{fp} on physical output is also dependent on the CI. In any case, this allows us to approach our *physical model* as a simple combination (multiplication) of correction factors, each derived from a specific effect when compared to a default case (i.e., fixed, single focal point). Dependent and independent parameters were identified during preliminary tests (not reported here), but our evaluation covers arbitrary combinations of all parameters, validating these assumptions and also the general correctness of our *physical model*.

4.1.3 *Characterization of Physical Effects.*

- Non-linear effects: Non-linear effects depend on CI alone. Thus we tested 5 different values of CI between 544 and 6531 Pa (3 repetitions, for a total of 15 samples), keeping other parameters at their default values (i.e., N_{fp}=1 point, f_d=0 Hz, T=31°C).

Our results, shown in Figure 4.a, clearly illustrate the presence of non-linear behaviours. The response is reasonably linear for CI values < 2 KPa (green dashed line), showing good agreement between the *expected* pressure (CI) and the measured pressure. However, for higher CI values the PAT fails to deliver the pressure expected (i.e., actual pressure is lower than demanded CI).

This relationship can be fitted using a sigmoid function (orange continuous line in Figure 4.a), and the parameters fully defining function $NL(CI)$ can be found in Supplementary Material.

- Sub-optimum Driving Frequencies effects: This effect is caused by frequent changes in phase in each transducer, which increase the faster each point moves (f_d). Thus, we measured 9 different frequencies (f_d ={5, 10, 20, 40, 80, 120, 160, 240, 320 Hz}), retaining default values for CI=6531 Pa, N_{fp}=1 and T=31°C, and collecting 9 frequencies x 3 repetitions = 27 samples.

Our results are shown in Figure 4.b. As expected, the pressure delivered decreases significantly at higher frequencies (i.e., f_d>80 Hz). It is however surprising to see that the pressure delivered can exceed that of a static focal point at some frequencies (i.e., 5-40 Hz). This could be caused by a mismatch in the real-time clock of the PAT (e.g., its FPGA does not deliver *exactly* 40 KHz), due to transducer's resonance (i.e., actual frequency slightly higher than 40 KHz), or due to frequency shifts due to operating temperature. We repeated these tests 3 times and, whatever the cause, we can confirm this effect is consistently present every time.

This relationship between f_d and pressure can be fit with a 3rd degree polynomial equation $DF(f_d)$, with its specific parameters being provided in Supplementary Material.

- Temperature effects: Temperature effects only depend on T. We tested temperatures from 25°C to 50°C, in steps of 5°C, retaining CI=6.5 KPa, N_{fp}=1 point and f_d=0 Hz, collecting a total of 6x3 repetition = 18 samples.

Our results in Figure 4.c show a clear linear relationship between T and P_0. Delivered pressure decreases ~83 Pa for every degree increase (full parameters of $TT(T)$ in Supplementary Material).

- Power Limit effects: This effect comes into play when a device cannot deliver the intensities requested, either because the CI's are too high, or because it cannot deliver such CI for such a high number of points. To characterise this effect we measured combinations of 5 different CIs (range 544 Pa to 6.5 KPa) and 3 N_{fp} (1,2 or 3 points), for a total of 5 x 3 x 3 repetition = 45 measurements. The other parameters remained at f_d=0 Hz and T=31°C.

Our results show that, while the PAT can achieve intended pressures for any number of points at lower CIs (i.e., 544 and 1088 Pa), it cannot deliver CI=2721 Pa for N_{fp}=3; or any higher CIs for N_{fp} of 2 or 3 points. Fitting requires a more complex multi-variate cubic function $LP(CI, N_{fp})$, available in Supplementary Material.

4.1.4 *Evaluation of the Physical Model.*

We evaluated the ability of our *physical model* to predict the pressure the device would deliver under various combinations of CI, f_d, N_{fp} and T. More specifically, we tested our model's predictions against the data gathered for the tests in Section 4.1.3 (i.e. *training dataset*), but also against a *validation dataset*, exploring a broader range of combinations of parameters.

The latter *validation dataset* explored factorial combinations of: 5 different values of CIs (544 to 6531 Pa); N_{fp} including 1,2 or 3 points; and f_d including 11 frequencies (i.e., 9 prior frequencies between 5-320 Hz, plus 2 unseen frequencies 60 Hz and 200 Hz). During these tests, device temperature varied between 24.2 and 51.5 degrees, remaining very close to our intended operational range (i.e., 25-50°C). Thus, the *validation dataset* measured a total of 5 x 11 x 3 = 165 different STM stimuli, each at a variable temperature.

We test the accuracy of our model by looking at the relative error between our prediction and the actual measurement (i.e., absolute difference between predicted and measured, divided by the pressure measured). The relative error was 2.05% for our *training dataset*

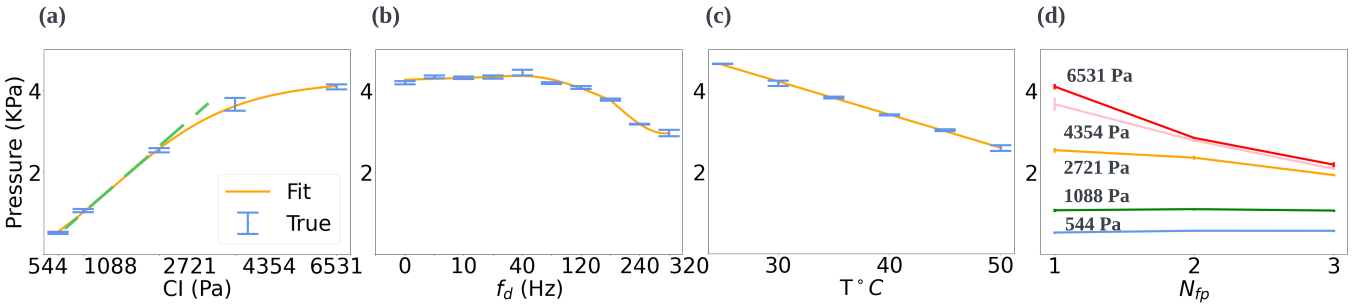

Figure 4: Characterization of physical effects: a) Effect of CI on acoustic pressure. b) Effect of f_d on acoustic pressure. c) Effect of Temperature on acoustic pressure. d) Effect of N_{fp} on the acoustic pressure of each focal point at 5 CIs.

and 7.8% (close to 6.49% obtained by [40]) for our *validation dataset* (i.e., detailed relative errors at each condition are available in Table 1 in Supplementary Material). We repeated this validation on a second OpenMPD device (i.e., see section C.2 in Supplementary Material), obtaining a relative error of 8.3% and confirming the trends observed for each physical effect (e.g., temperature being linear). This illustrates that, even if tuning might be required for each device, the general model could generalize to different devices.

This error from our model is in the same order of magnitude that the inherent error of the solver used (GS-PAT). That is, GS-PAT produces a mismatch of ~3% between the CI and the pressure delivered, even if an ideal PAT (free from any physical artefacts) could be used. Also, our error is smaller than the 12.2% JND pressure [42], suggesting that such differences would not be perceivable by users. This offers a stark contrast if no model was to be used (i.e., assume GS-PAT simulated pressure resemble real pressure), which would provide a relative error of ~102%, as detailed in Figure 3 in Supplementary Material.

4.2 STUDY 2: Minimum Perceivable Thresholds

Computing some of the parameters describing the physical stimuli (i.e., P_{MPT}, and F_{MPT}), required us to determine the MPT. We assume such thresholds will be independent of other parameters (e.g., N_{fp} and T), and explore $MPT(f_d)$ only as a function of f_d, which we derive from this user study.

4.2.1 *Experimental Design*.

We explored MPTs under nine different frequencies (f_d = 5, 10, 20, 40, 80, 120, 160, 240, and 320 Hz). In order to do this, we used a 1-up-1-down staircase design [4, 8, 40], interleaving individual steps from 2 staircases. The first staircase started from CI=1.5 KPa, decreasing CI with every step, while the second staircase started at the minimum CI=500 Pa value. Interweaving both staircases helped reduce predictability between current and the previous response, and provided more data (2 repetitions) for analysis.

In either case, participants were asked to answer if they perceived the stimulus (i.e., 'Yes' or 'No' answer), and we used a change of 3 dB in CI at each step, reducing it to 1 dB after three reversals [18, 40]. In order to reduce estimation bias, each staircase ran until at least eight reversals were obtained [53]. Please note, the initial staircase values (i.e., 1.5 KPa and 500 Pa) were selected from a pilot study, but this design allows testing of threshold values outside this range (e.g., if CI = 1.5 KPa is not felt, intensity would increase).

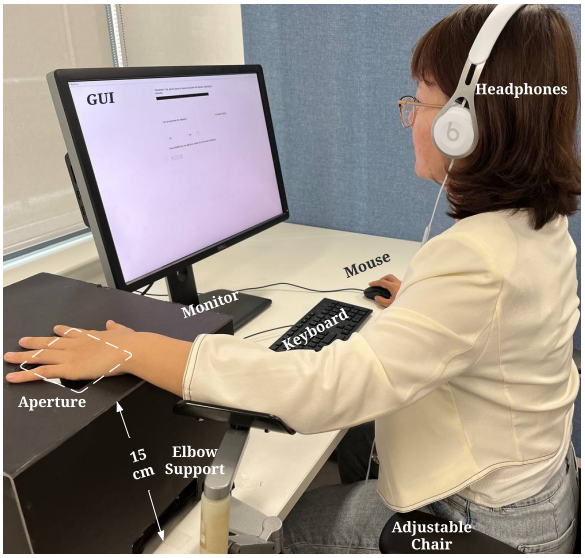

Figure 5: The overall experiment setup for study 2.

Each participant completed nine tests, one for each test frequency [18], counterbalanced using a Latin square design. The full experiment took a total of 90 minutes and each participant was compensated with £15 amazon voucher. Ethical approval was obtained from University College London's internal ethics committee and all participants gave informed consent (approval number: UCLIC_2021_014_ObristPE).

4.2.2 *Experimental setup and procedure*.

We reused the same platform used for Study 1 (OpenMPD software and hardware, with a temperature sensor). The PAT device was enclosed inside a black foam-made box covered with sound absorbing foam, and with a 10 cm by 10 cm square aperture on the top, so that the haptic stimuli could reach the participants' hands. The box also helped participants to align their hands above the device, keeping it at the right distance of 15 cm. An adjustable chair and elbow support were provided, adjusting them for the participant's

comfort, to avoid fatigue and to ensure they kept their hand still for the stimulation period.

Noise-canceling headphones playing pink noise were used to prevent participants from being affected by ambient noises and noise from the ultrasonic mid-air haptic device. Participants were required to use their dominant hand to interact with the mouse to record their responses through a GUI displayed on a 22" monitor in front of them. The overall experiment setup can be seen in Figure 5.

A total of 18 participants were recruited (9 females, mean age ±*SD*: 26.94±4.64), 6 of them with prior experience with UMH. After welcoming each participant into the room, the setup (i.e., box, elbow support and chair) was adjusted to the participant's needs. A prior temperature-taking process was taken on the participant's palm to ensure the temperature is above 35°C to reduce confounding factors. Each participant was asked to watch a video explaining the experiment procedure, tasks to complete, and instructions on using the GUI and report whether they could perceive the stimulus by answering 'yes' or 'no'. Moreover, participant responses and instructions were provided via the GUI. This ensured that all participants received the same information, minimizing potential biases introduced by the researcher's instructions.

Although related studies do not include any training sessions [9, 16, 40, 43], we included a staircase with f_d=5 Hz terminating after a single reversal as short training [18, 49]. This was followed by instructions to help participants become familiar with the testing and rating procedure. After training, participants were exposed to 9 tests (one per frequency), each featuring 2 interleaved staircases. After perceiving one stimulus in a staircase for 5 seconds, the GUI instructed the participants to enter whether they perceived the stimulus or not. This short duration of training, compared to the length of the whole study (i.e., 20 seconds vs an hour and half), should ensure minimum interference of training with the testing stage.

Two-minute breaks were scheduled after every 40 stimuli ratings, including a temperature-checking process to verify the participant's palm temperature remained above 35°C. Each stimulus was followed by a 5-second interval for users to provide their response, with no stimuli being delivered during this period of time. This aimed to reduce sensory bias [40], and to avoid enhancement effects (increased perceived magnitude of a stimulus due to prior stimuli decays to zero after approximately 500 ms [51]).

4.2.3 ***Results***.

After data collection, *CI* values were converted to P_0 pressures using our *physical model* and the average of each staircase's last 8 reversals was used to estimate the 50% *MPT* [53], with results summarized in Figure 6. We removed one outlier (i.e., response outside the 1.5∗interquartile range for that f_d). Results were normally distributed (Shapiro-Wilk, $p > .05$) but violated sphericity assumptions (Mauchly's test [36] with $p < .05$). Hence, we used Repeated measures ANOVA with Greenhouse-Geisser sphericity correction [15], and interpreted effect sizes using partial η^2 [7] and Holm-Bonferroni corrections [1], finding significant effects of f_d on *MPT* (f-value = 24.282, $p < 0.001$; partial $\eta^2 = 0.603$), justifying the use of f_d as a function parameter for our *MPT* function. Average

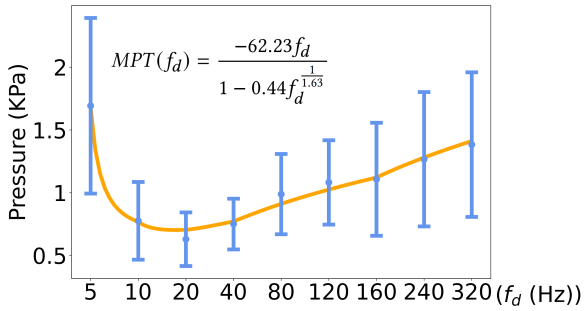

Figure 6: Effect of f_d on user's *MPT* in Pa. Mean and standard deviation of *MPT* across users shown in blue. The orange line display the fitting of our $MPT(f_d)$ function.

*MPT*s, their standard deviation for each f_d, and post-hoc results can be found in Tables 3 and 4 in Supplementary Material.

Participants showed maximum sensitivity (lowest *MPT*) when f_d is around 20 - 40 Hz, which is to be expected as these frequencies trigger Meissner and Pacinian corpuscles [27]. Also, such f_d's would translate to drawing speeds of 4 to 8 m/s, aligning with the findings in [11] and [55] that such speeds increase user's *PI*. Sensitivity decreased (i.e., higher *MPT*s) for higher frequencies, contradicting findings from AM stimulation [40] that 120Hz and 40Hz result in minimum and maximum *MPT*. This result suggests that humans perceive frequencies rendered by STM and AM differently.

The standard deviation of the *MPT* increases for 5, 120, 160, 240, and 320 Hz, frequencies to which participants are less sensitive (i.e., high *MPT* values). This indicates that users found it hard to provide a congruent rating for those frequencies, encouraging the use of 10 to 80 Hz as an optimum f_d range for multi-point STM.

Finally, this experiment allowed us to derive an analytical expression for our $MPT(f_d)$ function (shown in Figure 6), as well as to compute our 5 physical properties, introduced in related work and detailed in Supplementary Material.

5 PERCEPTUAL MODEL

The *Perceptual Model* aims to provide an estimate of users' response to multi-point STM, including both average *PI* and its standard error PI_{SE} (i.e., indicator of *spread*, or inter-subject variability). Study 3 describes a magnitude estimation study run to retrieve this information, describing both our findings, and the model produced (and the variables that better predict *PI*).

5.1 STUDY 3: Magnitude Estimation of *PI*

This section describes a magnitude estimation study looking into the *PI* reported by participants, as the input parameters of our multi-point STM technique varied (i.e., *CI*, f_d, N_{fp} and *T*).

5.1.1 ***Experimental Design***.

We created STM stimuli varying all input parameters, according to a full factorial design. More specifically, we reused the same nine frequencies f_d used for our prior studies. For each frequency, we tested 5 different values of *CI*, evenly distributed between $MPT(f_d)$ (i.e., minimum Pa perceptible to users for that f_d) and maximum *CI*

= 6.5 KPa. We also tested N_{fp} of 1, 2 or 3 points. Temperature (T) was monitored during the study, but is not an independent variable. We fixed the remaining STM modulation parameters in the same way than Study 1 (i.e., sampling rate of 100 points, height of 15 cm, circle diameter of 6.5 cm). Each stimuli was repeated 2 times, resulting in a total of 9 x 5 x 3 x 2 = 270 trials per participant.

We used a within-subjects experimental design and samples were presented in a pseudo-randomized order to each participant (i.e., reduce learning effects). Ethical approval was obtained from University College London's internal ethics committee and all participants gave informed consent (approval number: UCLIC_2021_014_ObristPE).

5.1.2 *Experimental setup and procedure*.

We re-used the same experimental setup used for Study 2, and recruited a total of 18 participants (9 females, mean age $\pm SD$: 31.72 ± 10.33), 7 of them with prior experience with UMH.

After welcoming each participant into the room, the setup was adjusted to the participant's needs (i.e., box, elbow support and chair) and an introductory video was shown to the user, to explain the experiment procedure, GUI, tasks to complete and rating procedure. After being instructed, a fixed set of 5 training stimuli was used to help participants familiarize themselves with the stimuli, testing and rating procedures and to consolidate their rating scale (particularly important given the unbounded scale used for *PI*, which we explain below).

After training, each participant was presented with each of the 270 test stimuli. Users experienced each stimulus (i.e., a given combination of CI, N_{fp} and f_d) for 5 seconds, and reported their estimated value for PI using the GUI. PI was rated using the absolute magnitude estimation method [23, 40], following a user-defined scale from 0 to infinity, which was then normalized between 0 and 1, allowing us to compare results with previous studies using the same metric [11, 12, 45, 55]. Regular 1 minute breaks were provided every 40 trials, and the overall duration of the experiment was 40 minutes. At the end of the experiment, each participant received a £10 amazon gift card for their participation.

5.2 Results: Multi-point STM effects on PI

We explored the effects on PI of our independent variables (i.e., CI, N_{fp}, f_d), but also of the physical properties derived from our *Physical Model* (i.e., P_0, P_{MPT}, F_0, $F_{2.1cm}$, F_{MPT}) on the optimum f_d range. For the first ones, we used Friedman's test (i.e., data was not normally distributed) and interpret effect sizes using Kendall's W Value [48]. The latter ones cannot be interpreted in this way (i.e., our physical properties are continuous variables), so we instead computed distance correlation coefficients (dcc) [46] between each property and PI. Such effects are summarized in Table 1.

Our results show that indeed all input variables (i.e., CI, N_{fp}, f_d) affect PI, confirming results from prior studies [11, 55]. Our results also show largest effects for CI (W = 0.656), followed by f_d (W = 0.065) and N_{fp} (W = 0.028).

These results indicate that the intensity of the stimuli (CI) bears most responsibility when determining PI. However, results from our *Physical Model* also showed how this is an unreliable metric to characterise the physical stimuli.

Table 1: The effect size of each STM parameter on perceived intensity and distance correlation coefficients between physical properties and perceived intensity under optimum f_d range.

10 - 80 Hz Parameters	Effect (W/dcc)
f_d	W = 0.065
N_{fp}	W = 0.028
CI	W = 0.656
P_0	dcc = 0.994
P_{MPT}	dcc = 0.995
$F_{2.1cm}$	dcc = 0.984
F_0	dcc = 0.981
F_{MPT}	dcc = 0.963

In order to explore if our physical properties could provide a better predictor for PI, we investigated the correlation between each physical property and perceived intensity (see dcc values in Table 1). This comparison shows that all the properties derived from our *physical model* provide very high correlation values, all becoming potentially good predictors for PI. Pressures seem to provide better prediction than forces. This is reasonable as pressure encodes both physical stimuli and area of contact and provides a more accurate representation of user's tactile experience. The inclusion of MPTs also improves (even if only slightly) prediction results. Among all 5 properties, P_{MPT} provided the most accurate results and we chose this property to continue to explore our *perceptual model*.

We built our model around the 4 variables identified: CI, P_{MPT} (as a potential replacement to CI), f_d and N_{fp}, by looking at the effect that introducing each of them has on our prediction accuracy.

Table 2: The Mean relative error of each model developed

10 - 80 Hz Parameters	$(PI)\%$	$PI_{SE}\%$
f_d	28.5	15.5
N_{fp}	28.6	15.8
CI	28.3	14.1
P_{MPT}	19.1	10.3
$P_{MPT} + f_d$	17.4	10.0
$P_{MPT} + N_{fp}$	11.9	10.1
$P_{MPT} + f_d + N_{fp}$	8.0	8.8

Table 2 summarizes the different models we tested, describing the variables considered (i.e, CI, P_{MPT}, f_d and N_{fp}), and reports the relative errors that we could achieve both to predict average PI (i.e., to model how strongly users' would perceive a STM stimuli) and standard error of PI (i.e., PI_{SE}, to model how differently users' would perceive it) above the MPT. In all cases, we limited our exploration to quadratic models. The way they were derived and the full analytical expression for each model can be found in Supplementary Material.

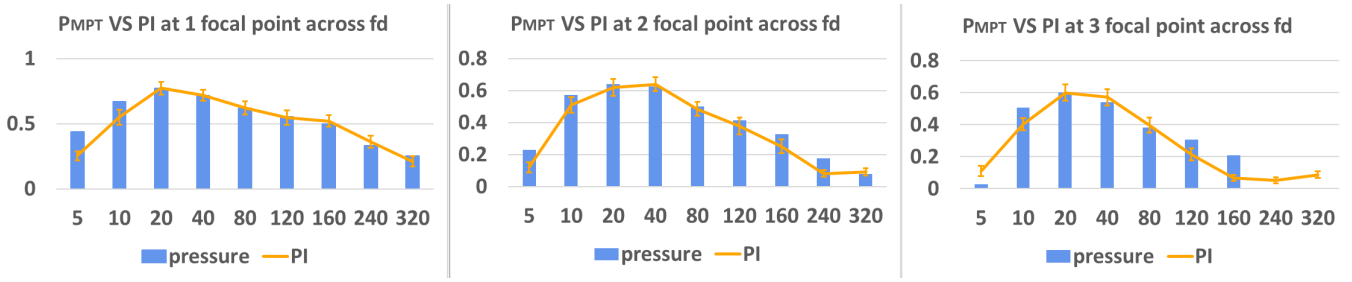

Figure 7: Relationship between PI and P_{MPT} per frequency range (f_d) and number of points (N_{fp}). The orange line shows average PI and standard error (whiskers) reported by users, while the blue bars represent the P_{MPT}, both normalized to a 0-1 range.

Looking first at the accuracy of models including a single variable (i.e., CI, P_{MPT}, f_d or N_{fp}), we can confirm that indeed P_{MPT} provide the highest prediction accuracy.

Figure 7 helps visualize the relative effects of such variable, by comparing users' PI to P_{MPT}, both normalized to a 0-1 range. The figure shows a very strong correlation between PI and P_{MPT}, but also how P_{MPT} provides higher errors for specific frequencies (e.g., high for f_d=5 Hz, or low for f_d = 80 Hz), pointing at perceptual effects related to other variables (e.g., f_d).

The figure also illustrates the low PI values achieved for frequencies outside the 10-80 Hz range, a result anticipated by our previous studies (i.e., weaker physical stimuli for higher frequencies from Study 1, and higher variance of MPTs from Study 2).

The next models in the table iteratively include additional variables (i.e., f_d and N_{fp}) on top of P_{MPT}, as a way to understand the gains from including additional parameters to the model. Including N_{fp} results reduces relative error to 11.9% and 10.0% for average PI and PI_{SE}, improving accuracy by 7.2% and 0.3% respectively, when compared to using P_{MPT} alone.

The inclusion of f_d, however, only results in very marginal gains (< 2% improved accuracy). This seems to indicate that such effect has already been included in the formation of P_{MPT}. That is, Study 1 showed how f_d affects the intensity of the stimuli, but this is a factor that is already captured by P_{MPT} and it seems P_{MPT} alone can mostly model such effects successfully.

Our final model, including all variables (i.e., P_{MPT}, f_d and N_{fp}) resulted in relative errors of 8.0% for average PI and 8.8% for PI_{SE}, and its overall fitting is shown in Figure 8 (See Tables 7 and 8 in the supplementary material for models' absolute and relative error at each optimum f_d across 1, 2, 3 N_{fp} for PI and PI_{SE} prediction.). Please notice that our results are comparable to other vibrotactile predictive models. Prior works [44, 54] indicated that an increase in amplitude tends to elevate the perceived intensity of vibrations according to Steven's power law. While these models require an expression for each frequency they consider, our model, however, allows predictions across a continuous frequency range (10-80 Hz). Although we applied different fitting functions, both of our perceived intensity prediction errors consistently fall within an acceptable range, specifically lesser than the tactile discrimination at 20% [5] mentioned in [54].

Figure 8 further reinforces the strong connection between the P_{MPT} and PI. The horizontal axis shows the P_{MPT} range that the STM stimuli in our study generated, showing how frequencies of 20 Hz and 40 Hz could achieve higher pressures. Unsurprisingly, those frequencies with higher P_{MPT} range also achieve higher PI's, indicating that the range of PI's an STM stimuli can generate is mostly related to the pressure it can deliver.

Supplementary Material explores this effect also for frequencies outside our range (e.g., 5 - 320 Hz), further showing how high-frequencies (which participants struggled to perceive) indeed provided stimuli with very low P_{MPT}. Hence, it will be hard to truly discern users' response to higher frequencies until devices become capable of accurately delivering these frequencies.

It worth noting that our most perceivable frequencies (20 Hz and 40 Hz) result in equivalent drawing speeds of 4 and 8 m/s, aligning with the results from Frier at al [11]. However, their observation that surface waves propagating on the skin were stronger could be the result of measuring a stronger stimuli, rather than simply the optimal drawing speeds that produced the phenomenon of constructive interference.

6 DISCUSSION

In this paper, we looked at the effects that various modulation parameters (CI, f_d, N_{fp}) have on multi-point STM, looking both at their effects on the physical stimuli (pressures and forces delivered) and on users' perceived intensity (PI). Our exploration helped us characterize 4 effects (i.e., *non-linear effects*, *limited power*, *sub-optimum driving frequencies* and *temperature*) affecting the physical stimuli delivered by the PAT device, and allowed us to derive a 2-stage model predicting users' average PI and standard error PI (variability from one users' response to another's). However, there are also limitations in our approach.

First of all, our model exploration was focused on identifying which variables provided a better predictive power to fit the results from our study. Further validation studies would be required to assess the generalizability of our model to real-world situations. Also, other variables such as different shapes [17, 31], locations on the skin (e.g., studies on forearm [38]), and sampling strategies [12] can be considered for generalization purpose.

While our perceptual model is constructed based on the universally producible physical properties of every UMH device, future works should continually validate and refine the model to ensure its robust applicability. While our use of open-source hardware and software make our results reproducible and directly applicable to the OpenMPD community, our model (i.e., the *physical model* and

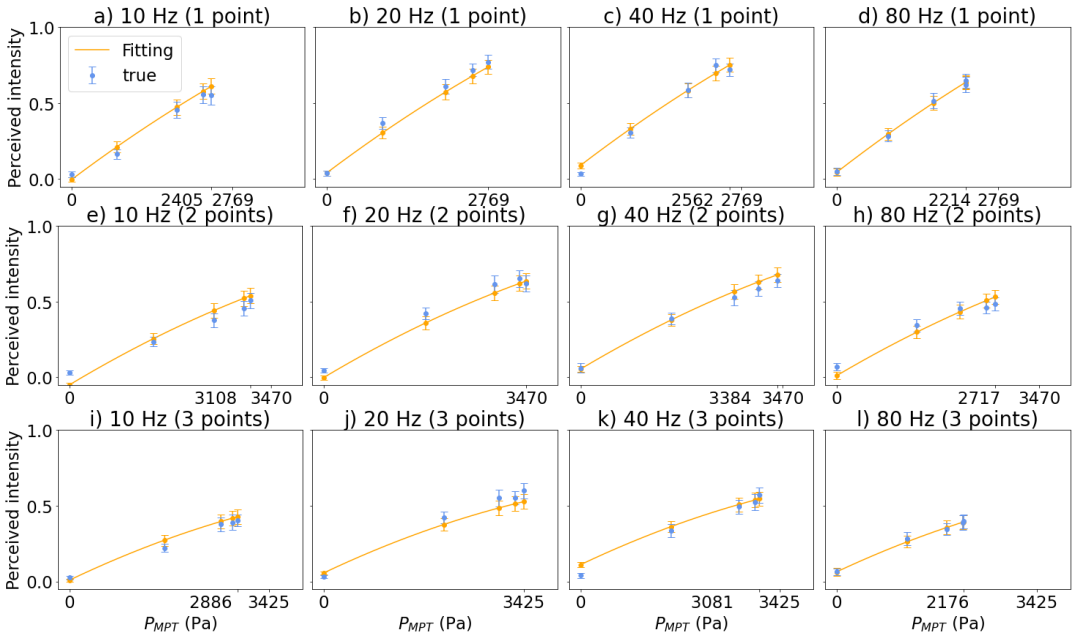

Figure 8: Relationship between P_{MPT} and perceived intensity under f_d from 10 to 80 Hz at 3 N_{fp} conditions. The error bars represent the standard error. The orange line represents the fitted *perceptual model*.

perceptual model) should be validated and revised in order to be used with other devices (e.g., Ultraleap or AUTD).

Finally, our model uses high-level parameters (f_d and N_{fp}) as proxies to assess the effect of phase changes (i.e., frequent phase changes are what cause *sub-optimum driving frequencies*). While it is useful for our purposes to use f_d and N_{fp} (i.e., they are inherent parameters for multi-point STM), works aiming to characterise PAT response in general should explore the effects of *sub-optimum driving frequencies* directly in terms of transducers' phase changes.

Even with these limitations, our work provides valuable insight to device manufacturers, haptic designers and HCI researchers.

Results from our *physical model* are particularly relevant for PAT manufacturers, as a first exploration of existing effects affecting the performance of PATs. Our model should be understood more like a high-level tool here and not a replacement for more accurate, low-level, physics-based models. However, even if not as accurate as those potential follow up models, and even if our *physical model* needs to be tuned for specific devices, the general trends identified for these physical effects will most likely hold.

This can help guide future efforts to improve devices. That is, improvements in temperature control will provide *linear* benefits (i.e., see *TT* factor), while benefits from improving *driving frequencies* are likely to be cubic (i.e., *DF* factor). Our model sets a preliminary scene to identify aspects requiring further exploration and where engineering solutions will be most benefitial.

Regarding *temperature* effects, monitoring would not be enough (i.e., compensating for temperature losses by increasing *CI* could lead to faster device heating). Accounting for temperature will require either active cooling or tuning techniques. Improving *driving frequencies* would require algorithms minimizing phase changes [20] , but these would need to be adapted to also cope with the high update rates required by STM [39, 41].

Our results can also be useful to haptic designers using multi-point STM in interactive design. Our results suggest constraining the multi-STM stimuli designed to 10-80 Hz, with stronger effects in the 20 - 40 Hz range. The ability to predict *PI* and the inter-subject variability (i.e., standard error of *PI*) can guide them to design stronger or more consistent stimuli, reducing the need for trial and error. The derived mapping has also provided the possibility of reverse prediction (achieve designed perceived intensity by finding required STM parameters to achieve essential physical property), providing a powerful tool for designing haptic interactions that are tailored to user expectations and preferences.

The predictivity in perceived intensity can further enhance the design of different level of stiffness sensation in UMH [33] from a physical perspective, and precisely provide various pulse profiles and thus enhance pulse training surgeries [24, 25]. From an entertainment perspective, our model can significantly enrich the movie-watching experiences by synchronizing haptic feedback to match the intensity of visual content [3]. This is particularly advantageous for multi-point stimuli, which enables complex shape rendering, thus allowing for a more advanced visual-haptic content synchronization. Similarly, our model opens opportunities to enhance haptic gaming experiences in the gaming industry by offering a diverse range of adjustable intensity feedback [14, 26].

Relevant implications can also be derived for HCI researchers. Our modelling procedure revealed how humans perceive haptic stimuli (i.e., both physical stimuli and MPT matters) and the physical properties that affect the user's perceptions. This encourages researchers in the haptic domain to follow similar procedures in

optimizing their models by finding the most relevant physical properties. Our model enhanced accurate stimuli delivery and perceptual response predictability. We showed that prior investigations in STM parameters' effects were limited, as some of the differences found could simply be due to uncontrolled factors (e.g., temperature). These factors often resulted in stimuli that were not physically comparable, leading to variations in pressure/force. Consequently, the observed differences between stimuli may have been influenced by these variables rather than the intended parameter variations. Our model, however, incorporates these factors, characterizes their effects, and then uses them to predict users' perceptual responses.

Our findings generally align with results from prior studies, but our look into the physical properties of the underlying stimuli might point towards alternative explanations to those suggested before. For instance, while we can confirm results from Frier at al. [11] that speeds of 5 to 8 m/s maximize user's perceived intensity (i.e., these speeds correspond to f_d range around 20 - 40 Hz in our Study 3), this effect could also be justified by the fact that devices' output was higher within this range (see Figure 7). Revisiting these results might be required, providing accurate characterization of the physical stimuli that are being compared. Researchers in this space should remain aware of PAT's poor performance at higher frequencies, and characterization of such higher frequency range might need to wait until delivery solutions are found.

In general, *PI* ratings seem more dependant on the physical properties of the stimuli, than on perceptual responses. Physical parameters can act as replacements of STM parameters (i.e., *CI*), improving overall accuracy, and the gains from considering f_d are relatively smaller. This does not mean perceptual responses are not important. Our best predictor (P_{MPT}) depended on values related to users' responses ($MPT(F_d)$), and modelling f_d and N_{fp} still provided benefits. However, as a community, we should avoid biases towards attributing observed effects to perceptual responses and be careful to also assess underlying physical effects.

7 CONCLUSION

We presented an exploration on the effects of various modulation parameters (*CI*, f_d, N_{fp}) have on stimuli, both at a physical and perceptual level. We reported on 3 different studies, which allow us to derive a two stage model predicting *PI* (i.e., average values and standard error), as a combination of a *physical* and a *perceptual model*.

Through our *physical model*, we identified and characterised 4 physical effects (*non-linear effects*, *limited power*, *sub-optimum driving frequencies* and *temperature*), being able to predict their effects on acoustic pressure with a relative error of 7.8% and thus, 5 different physical properties (i.e., P_0, P_{MPT}, F_0, $F_{2.1cm}$ and F_{MPT}).

Through our *perceptual model*, we could confirm how the physical intensity of the stimuli is the main effect influencing users' *PI*, above *perceptual* parameters such as f_d or N_{fp}. We can confirm that any of the physical properties proposed provides strong correlation with *PI* (i.e., supporting assumptions made in prior studies [10, 39, 55]), with P_{MPT} standing as a slightly better predictor for our scope (i.e., 1-3 points, 10-80 Hz). We combine all this in a final *perceptual model* combining all variables and resulting in a prediction error of 8.0% and 8.8% for average *PI* and standard error of *PI* respectively. We finally derive recommendations for manufacturers, haptic designers and HCI researchers exploring multi-point STM stimulation.

ACKNOWLEDGMENTS

This project has received funding from the European Union's Horizon 2020 research and innovation programme under grant agreement No 101017746, project Touchless.

REFERENCES

[1] Hervé Abdi. 2010. Holm's sequential Bonferroni procedure. *Encyclopedia of research design* 1, 8 (2010), 1–8. https://personal.utdallas.edu/~Herve/abdi-Holm2010-pretty.pdf

[2] Damien Ablart, William Frier, Hannah Limerick, Orestis Georgiou, and Marianna Obrist. 2019. Using Ultrasonic Mid-Air Haptic Patterns in Multi-Modal User Experiences. In *2019 IEEE International Symposium on Haptic, Audio and Visual Environments and Games (HAVE)* (Subang Jaya, Malaysia). IEEE Press, 1–6. https://doi.org/10.1109/HAVE.2019.8920969

[3] Damien Ablart, Carlos Velasco, and Marianna Obrist. 2017. Integrating Mid-Air Haptics into Movie Experiences. In *Proceedings of the 2017 ACM International Conference on Interactive Experiences for TV and Online Video* (Hilversum, The Netherlands) *(TVX '17)*. Association for Computing Machinery, New York, NY, USA, 77–84. https://doi.org/10.1145/3077548.3077551

[4] Carlo Aleci. 2021. Nonparametric Adaptive Psychophysical Procedures. In *Measuring the Soul*. EDP Sciences, 45–68.

[5] Seungmoon Choi and Katherine J. Kuchenbecker. 2013. Vibrotactile Display: Perception, Technology, and Applications. *Proc. IEEE* 101, 9 (2013), 2093 – 2104. https://doi.org/10.1109/JPROC.2012.2221071

[6] SUN Chongyang, NAI Weizhi, and SUN Xiaoying. 2019. Tactile sensitivity in ultrasonic haptics: Do different parts of hand and different rendering methods have an impact on perceptual threshold? *Virtual Reality & Intelligent Hardware* 1, 3 (2019), 265–275. https://doi.org/10.3724/SP.J.2096-5796.2019.0009

[7] J Cohen. 1988. edition 2. Statistical power analysis for the behavioral sciences. , 567 pages. https://doi.org/10.4324/9780203771587

[8] Tom N Cornsweet. 1962. The staircase-method in psychophysics. *The American journal of psychology* 75, 3 (1962), 485–491. http://www.jstor.org/stable/1419876

[9] Balkiss Friaa and Vincent Levesque. 2022. A Conceptual and Experimental Exploration of Electrovibration on the Palm and the Body. In *2022 IEEE Haptics Symposium (HAPTICS)*. IEEE, IEEE, 1–6. https://doi.org/10.1109/HAPTICS52432.2022.9765622

[10] William Frier, Abdenaceur Abdouni, Dario Pittera, Orestis Georgiou, and Rob Malkin. 2022. Simulating airborne ultrasound vibrations in human skin for haptic applications. *IEEE Access* 10 (2022), 15443–15456. https://doi.org/10.1109/ACCESS.2022.3147725

[11] William Frier, Damien Ablart, Jamie Chilles, Benjamin Long, Marcello Giordano, Marianna Obrist, and Sriram Subramanian. 2018. Using spatiotemporal modulation to draw tactile patterns in mid-air. In *International Conference on Human Haptic Sensing and Touch Enabled Computer Applications*. Springer, Springer, Cham, 270–281. https://doi.org/10.1007/978-3-319-93445-7_24

[12] William Frier, Dario Pittera, Damien Ablart, Marianna Obrist, and Sriram Subramanian. 2019. Sampling Strategy for Ultrasonic Mid-Air Haptics. In *Proceedings of the 2019 CHI Conference on Human Factors in Computing Systems* (Glasgow, Scotland Uk) *(CHI '19)*. Association for Computing Machinery, New York, NY, USA, 1–11. https://doi.org/10.1145/3290605.3300351

[13] M. Garcia-Rodriguez, J. Garcia-Alvarez, Y. Yañez, M.J. Garcia-Hernandez, J. Salazar, A. Turo, and J.A. Chavez. 2010. Low cost matching network for ultrasonic transducers. *Physics Procedia* 3, 1 (2010), 1025–1031. https://doi.org/10.1016/j.phpro.2010.01.132 International Congress on Ultrasonics, Santiago de Chile, January 2009.

[14] Orestis Georgiou, Craig Jeffrey, Ziyuan Chen, Bao Xiao Tong, Shing Hei Chan, Boyin Yang, Adam Harwood, and Tom Carter. 2018. Touchless haptic feedback for VR rhythm games. In *2018 IEEE Conference on Virtual Reality and 3D User Interfaces (VR)*. IEEE, IEEE, 553–554. https://doi.org/10.1109/VR.2018.8446619

[15] Samuel W Greenhouse and Seymour Geisser. 1959. On methods in the analysis of profile data. *Psychometrika* 24, 2 (1959), 95–112. https://doi.org/10.1007/BF02289823

[16] Xingwei Guo, Yuru Zhang, Wenxuan Wei, Weiliang Xu, and Dangxiao Wang. 2019. Effect of temperature on the absolute and discrimination thresholds of voltage on electrovibration tactile display. *IEEE transactions on haptics* 13, 3 (2019), 578–587. https://doi.org/10.1109/TOH.2019.2962111

[17] Daniel Hajas, Dario Pittera, Antony Nasce, Orestis Georgiou, and Marianna Obrist. 2020. Mid-air haptic rendering of 2D geometric shapes with a dynamic tactile pointer. *IEEE transactions on haptics* 13, 4 (2020), 806–817. https://doi.org/10.1109/TOH.2020.2966445

[18] Christian Hatzfeld, Siran Cao, Mario Kupnik, and Roland Werthschützky. 2016. Vibrotactile force perception–absolute and differential thresholds and external influences. *IEEE transactions on haptics* 9, 4 (2016), 586–597. https://doi.org/10.1109/TOH.2016.2571694

[19] Ryuji Hirayama, Diego Martinez Plasencia, Nobuyuki Masuda, and Sriram Subramanian. 2019. A volumetric display for visual, tactile and audio presentation using acoustic trapping. *Nature* 575, 7782 (2019), 320–323. https://doi.org/10.1038/s41586-019-1739-5

[20] Takayuki Hoshi. 2016. Gradual phase shift to suppress noise from airborne ultrasound tactile display. In *Proc. ACM CHI Workshop Mid-Air Haptics Displays: Syst. Un-instrumented Mid-Air Interact., Session 2: Provide Vis. Haptic Feedback*. 2 pages. https://www.hoshistar81.jp/pdf/2016CHI_MidairWS.pdf

[21] Takayuki Hoshi, Takayuki Iwamoto, and Hiroyuki Shinoda. 2009. Non-contact tactile sensation synthesized by ultrasound transducers. In *World Haptics 2009-Third Joint EuroHaptics conference and Symposium on Haptic Interfaces for Virtual Environment and Teleoperator Systems*. IEEE, IEEE, 256–260. https://doi.org/10.1109/WHC.2009.4810900

[22] Raphael Hover, Matthias Harders, and Gabor Szekely. 2008. Data-driven haptic rendering of visco-elastic effects. In *2008 Symposium on Haptic Interfaces for Virtual Environment and Teleoperator Systems*. IEEE, IEEE, 201–208. https://doi.org/10.1109/HAPTICS.2008.4479943

[23] Yu Huang and Michael J Griffin. 2014. Comparison of absolute magnitude estimation and relative magnitude estimation for judging the subjective intensity of noise and vibration. *Applied Acoustics* 77 (2014), 82–88. https://doi.org/10.1016/j.apacoust.2013.10.003

[24] Gary MY Hung, Nigel W John, Chris Hancock, Derek A Gould, and Takayuki Hoshi. 2013. UltraPulse-simulating a human arterial pulse with focussed airborne ultrasound. In *2013 35th Annual International Conference of the IEEE Engineering in Medicine and Biology Society (EMBC)*. IEEE, IEEE, 2511–2514. https://doi.org/10.1109/EMBC.2013.6610050

[25] Gary MY Hung, Nigel W John, Chris Hancock, and Takayuki Hoshi. 2014. Using and validating airborne ultrasound as a tactile interface within medical training simulators. In *International Symposium on Biomedical Simulation*. Springer, Springer, Cham, 30–39. https://doi.org/10.1007/978-3-319-12057-7_4

[26] Inwook Hwang, Hyungki Son, and Jin Ryong Kim. 2017. AirPiano: Enhancing music playing experience in virtual reality with mid-air haptic feedback. In *2017 IEEE world haptics conference (WHC)*. IEEE, Publisher: IEEE, 213–218. https://doi.org/10.1109/WHC.2017.7989903

[27] Roland S Johansson and J Randall Flanagan. 2009. Coding and use of tactile signals from the fingertips in object manipulation tasks. *Nature Reviews Neuroscience* 10, 5 (2009), 345–359. https://doi.org/10.1038/nrn2621

[28] Brian Kappus and Ben Long. 2018. Spatiotemporal modulation for mid-air haptic feedback from an ultrasonic phased array. *The Journal of the Acoustical Society of America* 143, 3 (2018), 1836–1836. https://doi.org/10.1121/1.5036027

[29] Bruel & Kjaer. 2008. *1/8" Pressure-field Microphone Type 4138 Datasheet*. Bruel & Kjaer. Available at https://kiptm.ru/images/Production/bruel/table_pdf/microphones_preamps/2017.02/4138.pdf.

[30] Sashidharan Komandur, Peter W Johnson, Richard L Storch, and Michael G Yost. 2009. Relation between index finger width and hand width anthropometric measures. In *2009 Annual International Conference of the IEEE Engineering in Medicine and Biology Society* (Minneapolis, MN, USA). IEEE, IEEE, 823–826. https://doi.org/10.1109/iembs.2009.5333195

[31] Benjamin Long, Sue Ann Seah, Tom Carter, and Sriram Subramanian. 2014. Rendering volumetric haptic shapes in mid-air using ultrasound. *ACM Trans. Graph.* 33, 6, Article 181 (nov 2014), 10 pages. https://doi.org/10.1145/2661229.2661257

[32] Robert Malkin, Brian Kappus, Benjamin Long, and Adam Price. 2023. On the non-linear behaviour of ultrasonic air-borne phased arrays. *Journal of Sound and Vibration* 552 (2023), 117644. https://doi.org/10.1016/j.jsv.2023.117644

[33] Maud Marchal, Gerard Gallagher, Anatole Lécuyer, and Claudio Pacchierotti. 2020. Can stiffness sensations be rendered in virtual reality using mid-air ultrasound haptic technologies?. In *International Conference on Human Haptic Sensing and Touch Enabled Computer Applications*. Springer, Springer, Cham, Cham, 297–306. https://doi.org/10.1007/978-3-030-58147-3_33

[34] Jonatan Martinez, Adam Harwood, Hannah Limerick, Rory Clark, and Orestis Georgiou. 2019. Mid-air haptic algorithms for rendering 3D shapes. In *2019 IEEE International Symposium on Haptic, Audio and Visual Environments and Games (HAVE)* (Subang Jaya, Malaysia). IEEE, IEEE Press, 1–6. https://doi.org/10.1109/HAVE.2019.8921211

[35] Asier Marzo and Bruce W. Drinkwater. 2019. Holographic acoustic tweezers. *Proceedings of the National Academy of Sciences* 116, 1 (2019), 84–89. https://doi.org/10.1073/pnas.1813047115

[36] John W. Mauchly. 1940. Significance Test for Sphericity of a Normal n-Variate Distribution. *The Annals of Mathematical Statistics* 11, 2 (1940), 204–209. http://www.jstor.org/stable/2235878

[37] Marianna Obrist, Sue Ann Seah, and Sriram Subramanian. 2013. Talking about Tactile Experiences. In *Proceedings of the SIGCHI Conference on Human Factors in Computing Systems* (Paris, France) *(CHI '13)*. Association for Computing Machinery, New York, NY, USA, 1659–1668. https://doi.org/10.1145/2470654.2466220

[38] Dario Pittera, Orestis Georgiou, Abdenaceur Abdouni, and William Frier. 2022. "I Can Feel It Coming in the Hairs Tonight": Characterising Mid-Air Haptics on the Hairy Parts of the Skin. *IEEE Transactions on Haptics* 15, 1 (2022), 188–199. https://doi.org/10.1109/TOH.2021.3110722

[39] Diego Martinez Plasencia, Ryuji Hirayama, Roberto Montano-Murillo, and Sriram Subramanian. 2020. GS-PAT: high-speed multi-point sound-fields for phased arrays of transducers. *ACM Transactions on Graphics (TOG)* 39, 4 (2020), 138–1. https://doi.org/10.1145/3386569.3392492

[40] Ahsan Raza, Waseem Hassan, Tatyana Ogay, Inwook Hwang, and Seokhee Jeon. 2020. Perceptually Correct Haptic Rendering in Mid-Air Using Ultrasound Phased Array. *IEEE Transactions on Industrial Electronics* 67, 1 (2020), 736–745. https://doi.org/10.1109/TIE.2019.2910036

[41] Antonio Montano Murillo Roberto, Hirayama Ryuji, and Diego Martinez Plasencia. 2022. OpenMPD: A low-level presentation engine for Multimodal Particle-based Displays. *Transaction on Graphics* 42, 2, Article 24 (apr 2022), 12 pages. https://doi.org/10.1145/3572896

[42] Isa Rutten, William Frier, and David Geerts. 2020. Discriminating Between Intensities and Velocities of Mid-Air Haptic Patterns. In *Haptics: Science, Technology, Applications*, Ilana Nisky, Jess Hartcher-O'Brien, Michaël Wiertlewski, and Jeroen Smeets (Eds.). Springer International Publishing, Cham, 78–86. https://doi.org/10.1007/978-3-030-58147-3_9

[43] Yatharth Singhal, Haokun Wang, Hyunjae Gil, and Jin Ryong Kim. 2021. Mid-Air Thermo-Tactile Feedback using Ultrasound Haptic Display. In *Proceedings of the 27th ACM Symposium on Virtual Reality Software and Technology* (Osaka, Japan) *(VRST '21)*. Association for Computing Machinery, New York, NY, USA, Article 28, 11 pages. https://doi.org/10.1145/3489849.3489889

[44] Stanley S Stevens. 1957. On the psychophysical law. *Psychological review* 64, 3 (1957), 153. https://doi.org/10.1037/h0046162

[45] Paul Strohmeier and Kasper Hornbæk. 2017. Generating Haptic Textures with a Vibrotactile Actuator. In *Proceedings of the 2017 CHI Conference on Human Factors in Computing Systems* (Denver, Colorado, USA) *(CHI '17)*. Association for Computing Machinery, New York, NY, USA, 4994–5005. https://doi.org/10.1145/3025453.3025812

[46] Gábor J. Székely, Maria L. Rizzo, and Nail K. Bakirov. 2007. Measuring and testing dependence by correlation of distances. *The Annals of Statistics* 35, 6 (2007), 2769 – 2794. https://doi.org/10.1214/009053607000000505

[47] Ryoko Takahashi, Keisuke Hasegawa, and Hiroyuki Shinoda. 2018. Lateral Modulation of Midair Ultrasound Focus for Intensified Vibrotactile Stimuli. In *Haptics: Science, Technology, and Applications*, Domenico Prattichizzo, Hiroyuki Shinoda, Hong Z. Tan, Emanuele Ruffaldi, and Antonio Frisoli (Eds.). Springer International Publishing, Cham, 276–288. https://doi.org/10.1007/978-3-319-93399-3_25

[48] Maciej Tomczak and Ewa Tomczak. 2014. The need to report effect size estimates revisited. An overview of some recommended measures of effect size. *Trends in Sport Sciences* 1 (2014), 19. https://cir.nii.ac.jp/crid/1371694592362914690

[49] M. Y. Tsalamlal, N. Ouarti, and M. Ammi. 2013. Psychophysical study of air jet based tactile stimulation. In *2013 World Haptics Conference (WHC)*. IEEE, 639–644. https://doi.org/10.1109/WHC.2013.6548483

[50] Vaishali Upadhye and Sudhir Agashe. 2016. Effect of Temperature and Pressure Variations on the Resonant Frequency of Piezoelectric Material. *Measurement and Control* 49, 9 (2016), 286–292. https://doi.org/10.1177/0020294016663974 arXiv:https://doi.org/10.1177/0020294016663974

[51] Ronald T Verrillo and George A Gescheider. 1975. Enhancement and summation in the perception of two successive vibrotactile stimuli. *Perception & Psychophysics* 18, 2 (1975), 128–136. https://doi.org/10.3758/BF03204100

[52] Mickeal Verschoor, Dan Casas, and Miguel A. Otaduy. 2020. Tactile rendering based on skin stress optimization. *ACM Trans. Graph.* 39, 4, Article 90 (aug 2020), 13 pages. https://doi.org/10.1145/3386569.3392398

[53] G. B. Wetherill. 1963. Sequential Estimation of Quantal Response Curves. *Journal of the Royal Statistical Society. Series B (Methodological)* 25, 1 (1963), 1–48. http://www.jstor.org/stable/2984541

[54] Yongjae Yoo, Inwook Hwang, and Seungmoon Choi. 2022. Perceived Intensity Model of Dual-Frequency Superimposed Vibration: Pythagorean Sum. *IEEE Transactions on Haptics* 15, 2 (2022), 405–415. https://doi.org/10.1109/TOH.2022.3144290

[55] Shen Zhouyang, Vasudevan Madhan, Kumar, Kučera Jan, Obrist Marianna, and Plasencia Diego, Martínez. 2023. Multi-point STM: Effects of Drawing Speed and Number of Focal Points on Users' Responses using Ultrasonic Mid-Air Haptics. In *Proceedings of the 2023 CHI Conference on Human Factors in Computing Systems*. Association for Computing Machinery, New York, NY, USA, 565–578. https://doi.org/10.1145/3544548.3580641